Proceedings of the 15th International Heat Transfer Conference, IHTC-15
August 10-15, 2014, Kyoto, Japan

IHTC15-8268

ABSORPTION OF SHORT-PULSED LASER RADIATION IN SUPERFICIAL HUMAN TISSUES: TRANSIENT VS QUASI-STEADY RADIATIVE TRANSFER

Jaona H. Randrianalisoa[1*], Leonid A. Dombrovsky[2], Wojciech Lipiński[3], Victoria Timchenko[4]

[1] GRESPI, Univer. de Reims Champagne-Ardenne, EA 4694, Moulin de la Housse, F-51687, Reims, France
[2] Joint Institute for High Temperatures, Krasnokazarmennaya 17A, NCHMT, 111116, Moscow, Russia
[3] Research School of Engineering, Australian National University, Canberra, ACT 0200, Australia
[4] School of Mech. and Manufact. Engineering, University of New South Wales, Sydney 2052, Australia

ABSTRACT

Transient radiative transfer effects are pertinent to thermal treatment of superficial cancer via short-pulsed laser irradiation. The transient effects become particularly important due to relatively strong scattering and long attenuation path of radiation in human tissues in the therapeutic window until the complete absorption. Our analysis is based on transport approximation for scattering phase function and the Monte Carlo method for radiative transfer. One-dimensional radiative transfer problem is considered, which was proved to be applicable for simulation of heat transfer and thermal destruction of tumors in superficial human tissues in the case of indirect heating strategy. A series of Monte Carlo calculations enables us to find the threshold of the steady-state approach applicability. In the biomedical problem under consideration, the steady-state solution for absorbed radiation power is sufficiently accurate at duration of laser pulse more than about 10 ps. The calculations for human tissues with embedded gold nanoshells, which are used to increase the local volumetric absorption of the radiation, showed that overheating of the nanoshells with respect to the ambient biological tissue is strongly dependent of the laser pulse duration. This effect is quantified for short pulses by solving the unsteady radiative transfer problem.

KEY WORDS: Radiation; Photon, phonon and electron transport; Bio-medical applications; Computational methods; Pulsed laser; Unsteady effects

1. INTRODUCTION

Thermal treatment of superficial cancer via short-pulsed radiation has been extensively studied in the last decade [1–3]. Visible and near-infrared laser radiation in the spectral range corresponding to the so-called therapeutic window, typically 0.6–1.4 μm [4, 5], is used for tumor heating in the direct (DHA) [6–8] and indirect (IHA) [9, 10] heating approaches. In IHA, an annular region around the tumor is irradiated and the tumor is heated predominantly by conduction during the time intervals between periodic laser irradiation. In both approaches, heating can be enhanced by embedding strongly absorbing gold nanoparticles (GNPs) [8, 11, 12]. IHA can also perform well without the use of GNPs [9, 10], alleviating the difficulties associated with nanoparticle supply and concentration control.

An accurate computational model for thermal treatment of superficial tumors by IHA must capture the relevant bio-heat transfer effects such as the metabolic heat generation, thermal non-equilibrium between arterial blood and ambient tissues and kinetics of the cell damage, as well as absorption of laser radiation in anisotropically scattering multi-layer human tissues. An approximate radiative transfer model with application to IHA [13] was examined by the authors in [14]. The transport approximation for the scattering phase function and differential models for radiative transfer [15, 16], in particular the modified two-flux

*Corresponding Author: jaona.randrianalisoa@univ-reims.fr

approximation [17], were shown to be sufficiently accurate at an acceptable computational cost. The study presented in [14] was based on a steady-state approach to radiative transfer, thus neglecting possible unsteady effects that may arise when very short pulses of the incident laser radiation are used.

Heat transfer in human tissues without GNPs or with GNPs remaining in thermal equilibrium with the ambient tissues can be analyzed using the radiation power absorbed in the tissues during a relatively long time as compared with the pulse duration. It should be noted that highly absorbing GNPs embedded in the tissue may not satisfy the thermal equilibrium condition in the case of very short laser pulses. But detailed study of this specific problem is beyond the scope of the present paper.

The problem of a transient radiative transfer has been addressed in numerous investigations, especially in the last decade [18–32]. However, only few of these studies were concerned with biomedical applications. To the best of our knowledge, there are no theoretical and computational studies in the literature concerning the problems related to interaction of short-pulsed radiation with human tissues containing embedded GNPs.

In this work, transient effects of radiative transfer in superficial human tissues during pulsed laser cancer treatment via IHA are considered in the limit where the finite speed of light is important due to very short pulse duration. Specifically, the objectives of this paper are: (1) to elucidate transient effects of radiative transfer in superficial human tissues including the case with embedded highly-absorbing GNPs subject to short-pulsed laser irradiation, and (2) to identify the limiting laser pulse duration for which the quasi-steady approach to radiative transfer in superficial human tissues remains valid.

2 PROBLEM STATEMENT

A schematic of an axisymmetric model superficial human tissue section during the thermal cancer treatment via IHA is shown in Fig. 1. The section includes five zones corresponding to different layers of human tissue (Fig. 1a), namely epidermis (#1), papillary and reticular dermis (#2), fat (#3), muscle (#4), and superficial tumor (#5). The light propagation in absorbing and scattering human tissues is modeled using a 3-D radiative transfer model. A 2-D section of the axisymmetric computational domain is shown in Fig. 1b. Since the external laser radiation does not typically reach the muscle layer even in the therapeutic window [9], only a part of this layer is included in the actual computational domain shown in Fig. 1b. The tumor is not directly irradiated in IHA, and thus it is excluded from the computational domain shown in Fig. 1b. Both zones should be included in their entirety in heat transfer models of superficial tissues undergoing long-time thermal treatment [9, 10, 13].

An annular region of the body surface A_{inc} surrounding the superficial tumor is exposed to short-pulsed laser irradiation. The irradiated area of the body surface is flat and optically smooth. This assumption is justified by a significant volumetric scattering of radiation in human tissues at very small effect of the reflection character on the volumetric radiation power absorbed in the tissues. Two variants are considered: (*i*) IHA with a specific type of gold nanoparticles consisting of a silica core enclosed in a gold shell, referred to as gold nanoparticles (GNPs) in the following text, embedded in an annular region (r_1=5 mm ≤ r ≤ r_2=10 mm, 0.1 mm ≤ z ≤ 2 mm) including parts of the dermis and fat layers, located underneath the plane of incidence of the laser beam, and (*ii*) IHA without GNPs.

For simplicity, it is assumed that for the variant with GNPs, their volume fraction is uniform in their suspension. Although the simulations are performed in the entire domain depicted in Fig. 1b, the absorbed radiative power is evaluated only for a cylindrical sub-domain of 3.5-mm thickness, 2.5-mm internal radius and 12.5-mm external radius, which includes parts of zones (#1)–(#3). The relatively small thickness of 3.5 mm is chosen based on the findings of [14] to elucidate the transient radiative transfer effects in the region of considerable absorption of laser radiation.

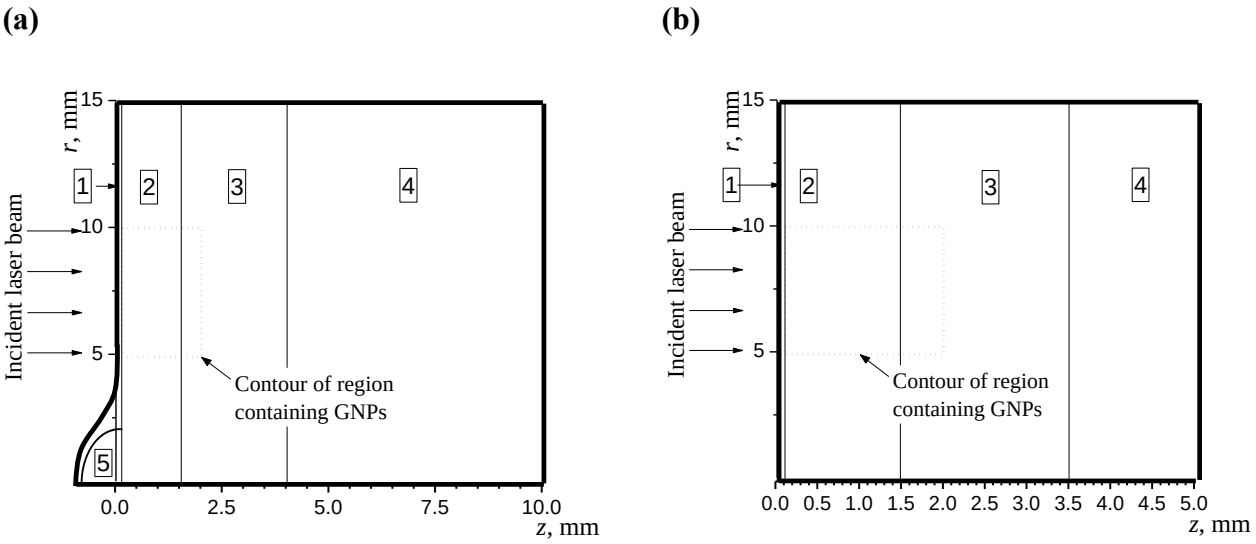

Fig. 1 Schematic of an axisymmetric problem with five zones corresponding to different tissue layers: (#1) epidermis, (#2) dermis, (#3) fat, (#4) muscle, and (#5) tumor: (a) 2-D tissue section including central, non-irradiated and annular irradiated regions; and (b) 2D view of the 3-D computational domain.

Separate computations are performed for a single pulse with Gaussian temporal shape and a train of Gaussian pulses given by [33],

$$q_{\mathrm{e}}(t) = q_{\mathrm{e,max}} \sum_{i=1}^{M} \exp\left[-4 \times \ln 2 \times \left(\frac{t - t_{\mathrm{c}} - (i-1)T_{\mathrm{p}}}{t_{\mathrm{p}}} \right)^2 \right] \tag{1}$$

where M is the number of pulses. The pulse is characterized by pulse maxima, $q_{\mathrm{e,max}}$, the width at half maximum, t_{p}, the time-shift of the first pulse maxima taken equal to $t_{\mathrm{c}} = 1.5t_{\mathrm{p}}$, and the pulse period, $6t_{\mathrm{p}}$, in the case of periodic pulse in accordance with parameters used in [33]. The Gaussian pulses $q_{\mathrm{e}}^{*}(t^{*}) = q_{\mathrm{e}}(t^{*}) / q_{\mathrm{e,max}}$ are plotted in Fig. 2 as a function of the relative time, $t^{*} = t / t_{\mathrm{p}}$.

The tissue index of refraction is assumed to be uniform in the computational region, $n_{\mathrm{t}} = 1.45$, even though its spatial variation in real multi-layered tissues has been reported in the range 1.34–1.45 [33]. The directional–hemispherical reflectivity of the tissue surface is obtained using Fresnel's equation for an interface between two non-absorbing media:

$$\rho_{\mu} = \frac{1}{2} \frac{\sin^2(\theta_{\mathrm{i}} - \theta_{\mathrm{t}})}{\sin^2(\theta_{\mathrm{i}} + \theta_{\mathrm{t}})} \left[1 + \frac{\cos^2(\theta_{\mathrm{i}} + \theta_{\mathrm{t}})}{\cos^2(\theta_{\mathrm{i}} - \theta_{\mathrm{t}})} \right] \qquad \sin\theta_{\mathrm{t}} = n_{\mathrm{t}} \sin\theta_{\mathrm{i}} \tag{2}$$

where θ_{i} and θ_{t} are the angles of incidence and transmission, respectively [34].

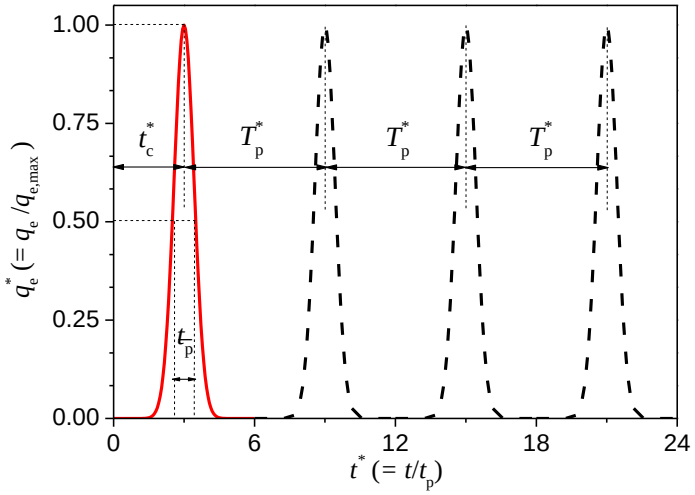

Fig. 2 The shape of a single pulse (solid curve) and a train of four pulses $q_e^*(t^*)$ used in the calculations.

Radiative properties of spherical GNPs are predicted using Mie theory [35], while the properties of biological tissues are retrieved from experimental studies reported in the literature [4, 5, 36]. The effects of finite time of light propagation over distances comparable with the size of GNPs are not considered. Applicability of this approach for GNPs of radius a is examined using the relation

$$t_p = 2an_t/c_0 \tag{3}$$

where c_0 is the speed of light in vacuum. For $a = 20\,\text{nm}$, we obtain $t_p \approx 2 \times 10^{-4}$ ps. Moreover, the time of light propagation for a distance equal to the wavelength, $t_\lambda = \lambda/c_0$, is about 0.03 ps at λ = 1 μm in vacuum. As a result, one can consider the interaction of a laser pulse with a single gold nanoparticle by assuming that the incident radiation is a plane wave with nearly-constant intensity at distances much greater than the particle size and invariant during the interaction process, justifying the use of Mie theory. It is also known that organelles inside human cells are responsible for the scattering properties of human tissues in the therapeutic window [4]. Application of Eq. (3) to organelles of size equal to the laser wavelength confirms that the scattering properties of human tissues are not affected by laser pulses for pulses longer than approximately 0.01 ps. Consequently, typical values of radiative properties of human tissues reported in the literature are employed in the present analysis.

The effects of extreme heating rates of GNPs are neglected in this study, and it is assumed that the temperature of GNPs, T_p, does not exceed a limiting value for explosive evaporation of water in the tissue surrounding the particle. According to [37], the maximum overheating of pure water at atmospheric pressure is equal to $\Delta T_{max} = T_p - T_s = 320\,\text{K}$, where T_s = 373 K is the water saturation temperature. The resulting formation of steam blankets around the GNP changes dramatically its radiative properties, and significantly affects heat transfer from GNPs to host tissue [15, 38].

The absorption and scattering coefficients of a tissue with embedded gold nanoshells of radius a and volume fraction f_v are calculated using [15],

$$\alpha = \alpha_t + \alpha_p \qquad \sigma_{tr} = \sigma_{tr,t} + \sigma_{tr,p} \tag{4a}$$

$$\alpha_p = 0.75 f_v \frac{Q_a}{a} \qquad \sigma_{tr,p} = 0.75 f_v \frac{Q_s^{tr}}{a} \tag{4b}$$

where Q_a and Q_s^{tr} are the absorption efficiency factor and the transport scattering efficiency factor, respectively [15]. According to the findings presented in [13], the following parameters of GNPs are used in the present study:

$$a = 20 \text{ nm} \qquad \delta = 0.725 \qquad Q_a = 7.828 \qquad Q_s^{tr} = 1.144 \tag{5}$$

where δ is the relative radius of the silica core.

3. QUASI-STEADY APPROACH

The quasi-steady radiative transfer model for non-uniform human tissues with embedded nanoparticles is presented in [14], and the mathematical details are omitted from this text for brevity. The transport approximation is employed for simplifying the anisotropic scattering of light inside human tissue. The mathematical problem is linear with respect to the incident radiative flux, and consequently the solution is obtained for the unit incident radiative flux.

3.1 Monte Carlo ray-tracing solution The Monte Carlo ray-tracing (MCRT) method for quasi-steady radiative transfer modeling is well-covered in the literature, e.g. [39, 40]. Thus, only the aspects specific to the present study are discussed here. The collision-based Monte Carlo (MC) method with the transport approximation to the scattering phase function is applied [14, 41]. The simulations are carried out for the total number of rays N_{ray}, with each ray of radiative power given by:

$$w_{q\text{-}s} = A_{inc}\bar{q}_e / N_{rays} \tag{6}$$

where $\bar{q}_e$ is the time-averaged irradiation flux by the laser, obtained as

$$\bar{q}_e = P(\tau)/\tau \qquad P(\tau) = \int_0^\tau q_e(t)dt \tag{7}$$

where τ is the laser pulse duration, $P(\tau)$ is the radiative energy per unit area of the laser pulse of total duration $\tau = 6t_p$ for a single pulse and $\tau = 6Mt_p$ for a train of M pulses. During tracing, rays undergo absorption and scattering in the medium, and boundary reflection and refraction. Rays are traced until they are absorbed inside the domain, exit the domain through the tissue surface, or propagate sufficiently far from the evaluation sub-domain discussed in the previous section. Rays incident at the tissue surface from within the medium are either transmitted or internally reflected, with the choice based on the actual value of the directional–hemispherical reflectivity given by Eq. (2). Rays propagating at large distances, here assumed at $r > 15$ mm and/or $z > 5$ mm, are considered as lost because of a low probability to be absorbed within the evaluation sub-domain.

The counters of absorbed rays are stored on a structured 2-D cylindrical mesh consisting of $n_z \times n_r = 50 \times 20$ annular cells with the following non-uniform spatial resolution:

$$\Delta z = \begin{cases} 0.01 \text{ mm} & \text{with } 0.0 \le z < 0.1 \text{ mm} \\ 0.07 \text{ mm} & \text{with } 0.1 \le z \le 1.5 \text{ mm} \\ 0.10 \text{ mm} & \text{with } 1.5 \le z \le 3.5 \text{ mm} \end{cases} \qquad \Delta r = 0.5 \text{ mm} \tag{8}$$

After tracing all N_{rays} rays, the normalized spatial distribution of the absorbed radiative power is obtained using [13]:

$$W^*(r,z) \approx (1-\rho_{\rm n})\frac{w_{\rm q-s}}{\bar{q}_{\rm e}}\frac{N_{\rm a}(i_{\rm z},i_{\rm r})}{V(i_{\rm z},i_{\rm r})}, \quad V(i_{\rm r},i_{\rm z}) = \frac{\pi \Delta z \Delta r^2}{4}\left[(i_{\rm r}+1)^2 - i_{\rm r}^2\right], \quad \rho_{\rm n} = \frac{(n_{\rm t}-1)^2}{(n_{\rm t}+1)^2} \tag{9}$$

where $V(i_{\rm r},i_{\rm z})$ and $N_{\rm a}(i_{\rm r},i_{\rm z})$ are the volume and number of rays absorbed in the cell $(i_{\rm r},i_{\rm z})$, respectively.

4. TRANSIENT APPROACH

The Monte Carlo ray-tracing (MCRT) method is selected as the method of solution for the unsteady radiative transfer problem in the non-uniform tissue to overcome numerical difficulties of deterministic solution methods applied to transient problems.

4.1 Transient MC algorithm The MC simulation of the unsteady problem is similar to the quasi-steady MC method described in Section 3. The main difference is that for unsteady problems, the histories of rays are evaluated at time instants and the time variation of radiative sources is taken into account during ray histories. In unsteady approach, each ray carry energy w defined by,

$$w = A_{\rm inc} P(\tau) / N_{\rm rays} \tag{10}$$

For a pulsed radiation (Fig. 2), the initial time, t_i, of the ray i for i =1 to $N_{\rm ray}$, is randomly sampled from the normalized Gaussian distribution:

$$R_{\rm t} = \int_0^{t_{\rm i}} q_{\rm e}(t)\,{\rm d}t \Big/ \int_0^{\tau} q_{\rm e}(t)\,{\rm d}t = \frac{P(t_i)}{P(\tau)} \tag{11}$$

with $P(t)$ already defined in Eq. (7).

During their paths, the rays may undergo volumetric absorption and scattering as well as boundary reflection and refraction. The determination of location and type of extinction and boundary interaction are managed in the same manner as for quasi-steady algorithm. At each extinction point, the time of flight of the ray is updated by adding the duration of the propagation of the last path before interaction $s_{\rm e}$:

$$t_{\rm e} = \frac{1}{c_0}\int_0^{s_{\rm e}} n_{\rm t}\,{\rm d}s \tag{12}$$

where $n_{\rm t}$ is the local refractive index of tissue. Consequently, the time at which the absorption of a ray i occurs is given by:

$$t = t_i + \sum_{j=1}^{m_{\rm S}+1} t_{{\rm e},j} \tag{13}$$

The sum in (13) is performed over the number of scattering events, $m_{\rm s}$, that the ray has undergone along its path before absorption.

At each absorption event, the number of absorbed rays at time t and space coordinates z and r is updated. In the computer code, the number of absorbed rays is stored in an array $N_{\rm a}(i_t,i_r,i_z)$, where i_t = int($t/\Delta t$) +1, i_r = int($r/\Delta r$) +1 and i_z = int($z/\Delta z$) +1 are the time and spatial indices, respectively. The absorbed power is calculated at n_t =100 equidistant time points, with the interval Δt. The spatial discretization of the computational domain is the same as in the quasi-steady approach of Section 3.

4.2 Transient absorbed power In the variant with GNPs, the thermal equilibrium between the GNPs and the ambient tissue is assumed in the macroscopic thermal model. This assumption is generally applicable for the irradiation by a continuous wave (cw) laser but it may be not correct in the case of a short-pulsed laser. In the thermal equilibrium approach, the absorbed power is determined from the number of rays absorbed in each computation cell without distinction of absorbing substances (GNP or tissue). Indeed, after all $N_{\rm rays}$ rays have been traced, the volumetric distribution of the transient absorbed power and the corresponding normalized quantity are approximated as:

$$W(t,r,z) \approx (1-\rho_{\mathrm{n}}) w \frac{N_a(i_{\mathrm{t}},i_{\mathrm{r}},i_{\mathrm{z}})}{\Delta t V(i_{\mathrm{r}},i_{\mathrm{z}})} \qquad W^*(t,r,z) = \tau\, W\big(t,r,z\big)/P\big(\tau\big) \tag{14}$$

which is applicable in the case of a relatively slow heating of the nanoparticles. Cooling of small particles by thermal conduction to the surrounding medium is rapid. The cooling time can be estimated using the solution for transient cooling of a homogeneous isothermal sphere with initial temperature $T_{\mathrm{p},0}$ placed in an infinite host medium at temperature T_{t}:

$$\frac{T_{\mathrm{p}} - T_{\mathrm{t}}}{T_{\mathrm{p},0} - T_{\mathrm{t}}} = \exp\big(-\mathrm{Fo}\big) \qquad \mathrm{Fo} = \frac{k_{\mathrm{t}} t}{(\rho c)_{\mathrm{p}} a^2} \tag{15}$$

In equation (15), k_{t} is the thermal conductivity of the host medium and $(\rho c)_{\mathrm{p}}$ is the specific volumetric heat capacity of the particle substance. The size of gold nanoshells is usually much smaller than the wavelength, referred to as the Rayleigh limit [13] consequently; the volumetric distribution of the absorbed radiation power in a particle is uniform. This justifies the isothermal approximation.

The Fourier number Fo is the only dimensionless parameter that determines the particle cooling rate. A condition of $\mathrm{Fo} = 1$ provides an estimate for the cooling time:

$$t_{\mathrm{c}} = (\rho c)_{\mathrm{p}} a^2 / k_{\mathrm{t}} \tag{16}$$

In the case of a gold nanoshell with a silica core, one can use the following relation:

$$(\rho c)_{\mathrm{p}} = (\rho c)_{\mathrm{s}} \delta^3 + (\rho c)_{\mathrm{g}} (1-\delta^3) \tag{17}$$

Substituting the values of $(\rho c)_{\mathrm{s}} = 1.99$ MJ m^{-3}K^{-1} for silica, $(\rho c)_{\mathrm{g}} = 2.51$ MJ m^{-3}K^{-1} for gold, and $k_{\mathrm{t}} = 0.445$ W/(m K) for dermis [20], one can obtain $t_{\mathrm{c}} \approx 2.1$ ns. This estimate shows that thermal nonequilibrium of the gold nanoshells and the surrounding tissue can be neglected for at least μs-long radiation pulses. For short-pulsed laser radiation with pulse width $t_{\mathrm{p}} << 2$ ns, the possible overheating of GNPs during the laser pulse should be taken into account.

When GNPs are exposed by a short-pulsed laser radiation, the temperature of a gold shell increases much faster (estimate heating time about 2 ps [42]) than that of surrounding tissue and has considerably greater temperature that that of ambient tissue during the time comparable to the laser pulse duration. In the microscale thermal model, the absorbed power by the gold shell of a nanoparticle and that by ambient tissue in each computational cell have to be determined. For a monochromatic incident radiation, the volumetric absorbed power by GNPs located within the computational cell i_{z} and at time point i_{t}, can be directly determined from the quantity $N_{\mathrm{a}}(i_{\mathrm{t}},i_{\mathrm{r}},i_{\mathrm{z}})$ by:

$$W_{\mathrm{p}}(t,r,z) \approx (1-\rho_{\mathrm{n}}) w \frac{\Psi(i_{\mathrm{r}},i_{\mathrm{z}}) N_{\mathrm{a}}(i_{\mathrm{t}},i_{\mathrm{r}},i_{\mathrm{z}})}{\Delta t V_{\mathrm{g}}(i_{\mathrm{r}},i_{\mathrm{z}})} \qquad \Psi(i_{\mathrm{r}},i_{\mathrm{z}}) = \alpha_{\mathrm{p}} / (\alpha_{\mathrm{p}} + \alpha_{\mathrm{t}}) \qquad V_{\mathrm{g}}(i_{\mathrm{r}},i_{\mathrm{z}}) = (1-\delta^3) f_{\mathrm{v}} V(i_{\mathrm{r}},i_{\mathrm{z}}) \tag{18}$$

with $\Psi(i_{\mathrm{r}},i_{\mathrm{z}})$ the probability for a ray to be absorbed by a GNP located at the radius *r* and abscissa *z*. $V_{\mathrm{g}}(i_{\mathrm{r}},i_{\mathrm{z}})$ the volume of gold shells contained within the cell of indexes i_{r} and i_{z}.

4.3 Time-averaged absorbed power It is convenient to introduce time-averaged absorbed powers, which indicate if the quasi-steady approach is applicable for calculations of the absorbed radiation power for the case of a pulsed irradiation of duration τ. The time-averaged absorbed power for use in macroscopic thermal equilibrium model can be obtained as follows:

$$\overline{W}^*(\tau_m, r, z) = \frac{1}{\tau_m}\int_0^{\tau_m} W^*(t, r, z)dt \qquad \tau_m \geq \tau \tag{19}$$

With τ_m the period over which the time resolved absorbed powers are averaged. For each pulse width, the value of τ_m is adjusted to determine the threshold from which the quasi-steady approach becomes applicable.

5. COMPUTATIONAL RESULTS

The optical properties of three human tissues at vacuum wavelength $\lambda = 0.6328\mu m$ are specified in Table 1. These data are taken from paper [9].

Table 1 Radiative properties of tissues in the computational region

Layer number	Tissue name	Layer thickness (mm)	α_t (1/mm)	$\sigma_{tr,t}$ (1/mm)
1	Epidermis	0.1	0.30	2.50
2	Dermis	1.4	0.27	3.75
3	Fat	2.0	0.19	2.70

5.1 Continuous irradiation The absorbed power results obtained from the 1-D modified two-flux approximation [14] at various volume fractions of gold nanoshells are presented in Fig. 3. The external radiation is absorbed mainly in a surface layer of irradiated medium and the absorbed specific power decreases with the distance from the illuminated surface. A local increase of volumetric absorption in the GNP suspension is observed at z = 0.1 mm. The referenced numerical solution along the laser beam axis at $r = (r_1 + r_2)/2$ obtained using the quasi-steady MC method at $f_v = 0$ and 2×10^{-6} is also shown in Fig. 3. A relative difference between two methods increases in the region of a very low absorption (at $z > 2$ mm), but only the important part of the referenced solution is shown. One can see very good agreement between approximate 1-D and exact solutions in the quasi-steady approach at least in the region of $z < 2$ mm. We will focus on the results for this important region in subsequent unsteady calculations.

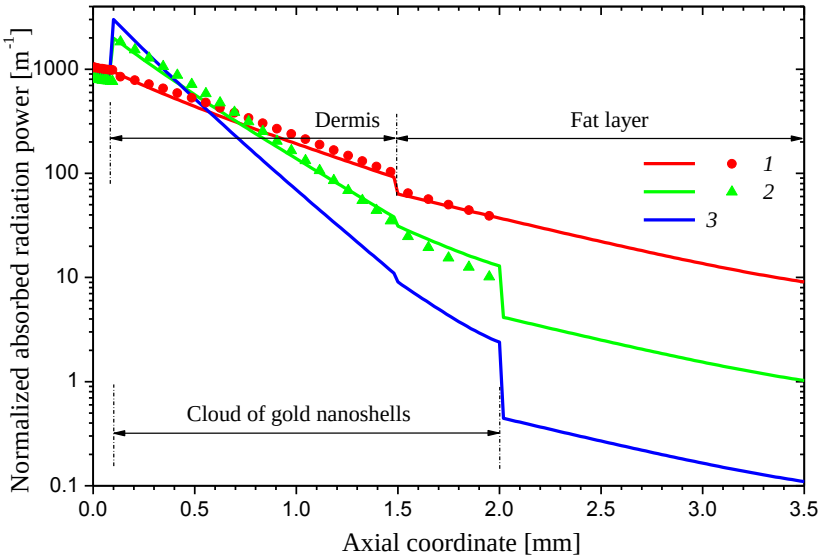

Fig. 3 Profiles of the normalized absorbed radiation power W^*: *1* – $f_v = 0$, *2* – $2\cdot10^{-6}$, *3* – $5\cdot10^{-6}$. Curves – results from the 1-D modified two-flux approximation; Symbols –MC results obtained along the laser beam axis at $r = (r_i + r_e)/2$.

5.2 Short-pulsed irradiation The variation of the time-averaged absorbed power along the laser beam axis at $r = (r_1 + r_2)/2$ for different pulse widths t_p is analyzed. The computational results are also compared with the traditional quasi-steady approach. Fig. 4a and 4b report the results for tissues with and without GNPs, respectively. The time-averaged results are calculated with an averaging period, τ_m, equal to the pulse duration τ. Both a single laser pulse and a train of 4 pulses were considered. It can be seen that for very short pulses ($t_p \leq 3$ ps), the time-averaged absorbed powers are only significant in a relatively small depth of the tissue ($z < 0.5$ mm). Indeed, the radiation does not finish propagating within the tissue layers during the time interval 0-τ due to strong scattering of light by human tissue. It means that the if the averaging period τ_m is constrained for example by the characteristic time for heat conduction at values less than tens of picoseconds, the quasi-steady approach is not applicable for very short pulses.

For long pulses ($t_p > 10$ ps), the deviation of the quasi-steady results with respect to the time-averaged results decreases. In these cases, the pulse durations ($\tau > 60$ ps for single pulses here) are relatively long for that the radiation can propagate in a large depth of the tissue ($z > 2$ mm). For the case of single pulse of width $t_p = 30$ ps and train of pulses of width $t_p = 10$ ps, the results from the quasi-steady and transient approaches are very close to each other. That means that the quasi-steady approach is applicable to calculate the absorbed power for the macroscopic thermal problem.

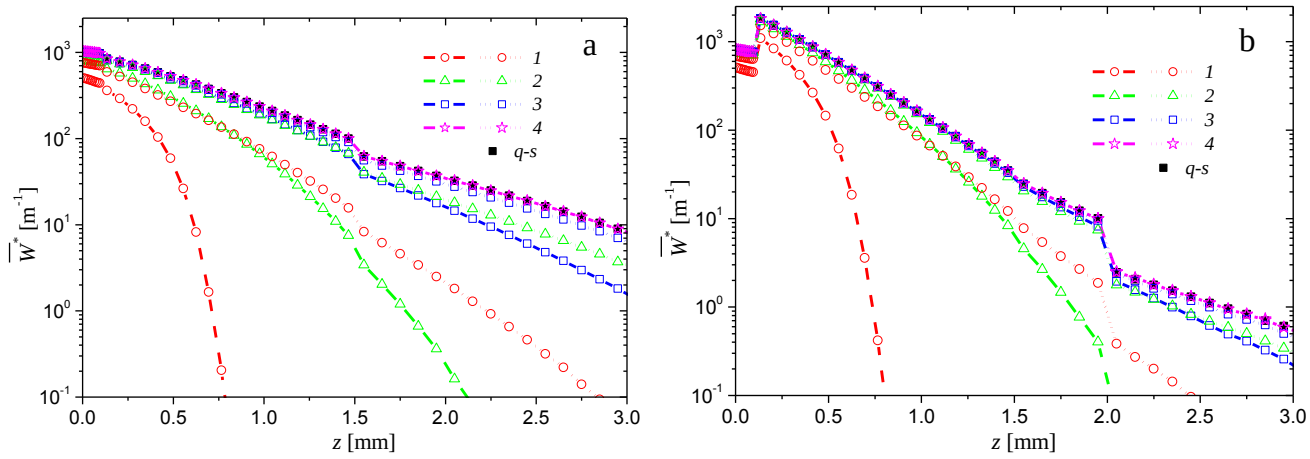

Fig. 4 Profiles of normalized absorbed radiation power $\overline{W}^*$ for a single pulse (dash curves with symbols) and a train of four pulses (dotted curves with symbols) at different t_p for the cases (a) with GNPs and (b) without GNPs: *1*– t_p =1 ps, *2* – 3 ps, *3* – 10 ps, *4* – 30 ps, *q-s* – quasi-steady solution.

Fig. 5 summarizes the value of τ_m corresponding to a relative deviation less than 5 % of the quasi-steady predictions with respect to the time-averaged results. This figure can be interpreted as follows. If the characteristic time for heat conduction is larger than τ_m, the quasi-steady approach is applicable otherwise; the transient approach should be used to determine the absorbed powers. For the particular case of a train of pulses, τ_m can be interpreted as the minimal time separating successive pulses, i.e. the pulse period, for that the quasi-steady approach is applicable.

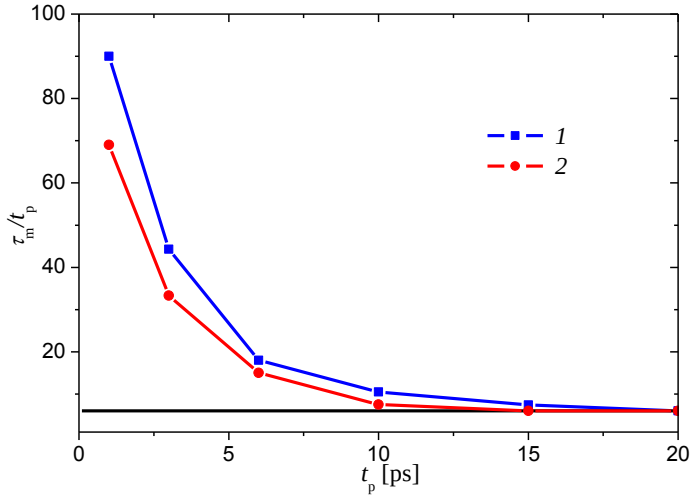

Fig. 5 Value of τ_m corresponding to a relative deviation less than 5 % of quasi-steady absorbed powers with respect to the time-averaged absorbed powers: *1* – case without GNPs; *2* – case with GNPs. Black line refers to the dimensionless single pulse duration $\tau/t_p = 6$ considered in this study.

5.3 Accuracy consideration In the MC method, the transient absorbed radiative power is obtained as an average result of ten independent runs. Each run consists of 5×10^7 rays and uses a unique seed for the random number generator. The computational time of a single run is about 5 min on a desktop computer Intel(R) Core(TM) i3-2330M CPU@ 2.2GHz processor with 4GB of RAM. The relative error is estimated by comparing the transient absorbed power obtained for $N_{ray}=10^7$, 5×10^7 and 5×10^8. The accuracy of the MC solution is quantified by computing a standard deviation based on the results of ten runs, each with Nrays/10 rays and a different value of the random number generator seed. Typical axial distributions of this relative error for a 1 ps pulse of laser radiation are presented in Fig. 6. Only the important part of the computational region characterized by a considerable value of the absorbed power is shown in this figure. In all cases, the relative error is less than 1% in the region of $z < 2$ mm, where the number of rays is sufficient to obtain accurate results. A non-uniform computational mesh used to obtain reliable numerical results was discussed in the recent paper [14].

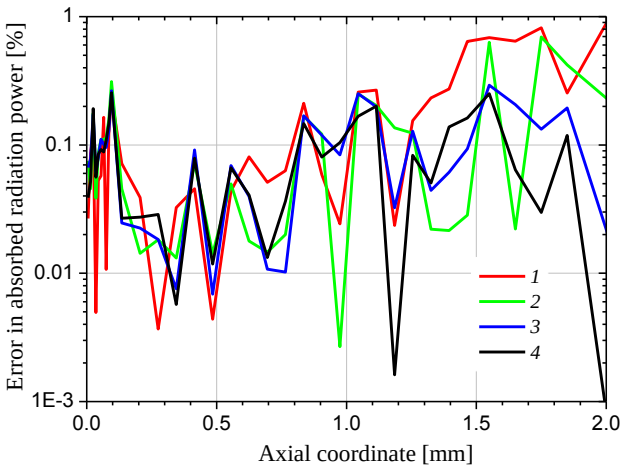

Fig. 6 Relative error in time-averaged absorbed radiation power at $r = (r_1+r_2)/2$ and different time moments for tissue subjected to a laser pulse of 1 ps width: *1* – τ_m = 14 ps, *2* – 22 ps, *3* – 30 ps, *4* – 200 ps.

6. CONCLUSIONS

The Monte Carlo method has been employed to analyze the effects of finite speed of light during the interaction of a short-pulsed laser radiation with human tissues as applied to thermal treatment of superficial tumors. The increase of the local radiation absorption in the tissue in the therapeutic window was examined for the short-pulsed radiation with gold nanoparticles (GNPs) embedded in human tissue. It was shown that the quasi-steady approach neglecting the final speed of light is applicable for human tissues without GNPs for laser pulse durations greater than 60 ps corresponding to a pulse width of 10 ps. At the same time, the microscale heat transfer in the vicinity of single GNPs is expected to be more sensitive to the duration of laser pulses because of considerable effect of overheating of these particles with respect to ambient tissue. The latter is considered as a subject of further studies

ACKNOWLEDGMENT

Leonid Dombrovsky is grateful for the partial financial support of this study from the Russian Foundation for Basic Research (Grant no. 13-08-00022a).

NOMENCLATURE

a	particle radius	(m)
A_{inc}	irradiated surface area	(m^2)
c_0	speed of light in vacuum	($m\ s^{-1}$)
d	thickness of dermis layer	(m)
f_{v}	volume fraction of particles	(–)
m_{s}	number of scattering events	
M	number of pulses	
n	real part of complex refractive index	
N	ray number	(–)
P	energy per unit area	($J\ m^{-2}$)
q	irradiation flux	($W\ m^{-2}$)
Q	efficiency factor (–)	
R	random number	(–)
s_{e}	free path of a ray until extinction	
t_{p}	pulse width	(s)
w	energy (rate) of ray bundles	(J) or (W)
W	volumetric absorbed power density	($W\ m^{-3}$)

Greek symbols

α	absorption coefficient	(m^{-1})
δ	relative radius of the silica core	
τ	laser pulse duration	(s)
τ_{m}	averaging time period	(s)
Ψ	probability of absorption	(–)

Subscripts and superscripts

a	absorbed
c	cooling
e	extinction, external irradiation
g	gold
i	initial time, incident
max	pulse maxima
n	normal to a surface
p	particle, pulse
qs	quasi-steady
ray	ray number
s	scattered, silica, saturation
t	tissue, time, transmitted
tr	transport
λ	spectral
*	normalized

REFERENCES

[1] Jiao, J. and Guo, Z. "Thermal interaction of short-pulsed laser focused beams with skin tissues," *Phys. Med. Biol*., 54(13), pp. 4225–4241, (2009).

[2] Huang, X., Kang, B., Qian, W., Mackey, M.A., Chen, P.C., Oyelere, A.K., El-Sayed, I.H., and El-Sayed, M.A., "Comparative study of photothermolysis of cancer cells with nuclear-targeted or cytoplasm-targeted gold nanospheres: continuous wave or pulsed lasers," *J. Biomed. Opt*., 15(5), paper 058002, (2010).

[3] Sajjadi, A.Y., Mitra, K., and Grace, M., "Ablation of subsurface tumors using an ultra-short pulse laser," *Opt. Lasers Eng*., 49(3), pp. 451–456, (2011).

[4] Mobley, J. and Vo-Dinh, T., "Optical properties of tissue," In Vo-Dinh T., Ed., "*Biomedical Photonics Handbook*", pp. 2-1–2-75, Boca Raton (FL): CRC Press, (2003).
[5] Tuchin, V.V., *Tissue Optics: Light Scattering Methods and Instruments for Medical Diagnosis, Second edition*, Vol. PM166, Bellingham (WA): SPIE Press, (2007).
[6] Niemz, M.H., *Laser-Tissue Interactions. Fundamentals and Applications. Second edition*, in "*Biological and Medical Physics Series*", Berlin: Springer, (2002).
[7] Vera, J. and Bayazitoglu, Y., "Gold nanoshell density variation with laser power for induced hyperthermia," *Int. J. Heat Mass Transf.*, 52(3–4), pp. 564–573, (2009).
[8] Huang, X. and El-Sayed, M.A., "Gold nanoparticles: Optical properties and implementations in cancer diagnosis and photothermal therapy," *J. Adv. Res*., 1(1), pp. 13–28, (2010).
[9] Dombrovsky, L.A., Timchenko, V., and Jackson, M., "Indirect heating strategy of laser induced hyperthermia: An advanced thermal model," *Int. J. Heat Mass Transf*., 55(17–18), pp. 4688–4700, (2012).
[10] Timchenko, V. and Dombrovsky, L., "Laser induced hyperthermia of superficial tumors: A transient thermal model for indirect heating strategy," *Comput. Therm. Sci*., 4(6), pp. 457–475, (2012).
[11] Khlebtzov, N.G. and Dykhman, L.A., "Optical properties and biomedical applications of plasmonic nanoparticles," *J. Quant. Spectr. Radiat. Transf*., 111(1), pp. 1–35, (2010).
[12] Bayazitoglu, Y., Kheradmand, S., and Tullius, T.K., "An overview of nanoparticle assisted laser therapy," *Int. J. Heat Mass Transf*., 67, pp. 469–486, (2013).
[13] Dombrovsky, L.A., Timchenko, V., Jackson, M., and Yeoh, G.H., "A combined transient thermal model for laser hyperthermia of tumors with embedded gold nanoshells," *Int. J. Heat Mass Transf*., 54(25–26), pp. 5459–5469, (2011).
[14] Dombrovsky, L.A., Randrianalisoa, J.H., Lipiński, W., and Timchenko, V., "Simplified approaches to radiative transfer simulations in laser induced hyperthermia of superficial tumors," *Comput. Therm. Sci*., 5(6), pp. 521–530, (2013).
[15] Dombrovsky, L.A. and Baillis, D., *Thermal Radiation in Disperse Systems: An Engineering Approach*, New York: Begell House, (2010).
[16] Dombrovsky, L.A. "The use of transport approximation and diffusion-based models in radiative transfer calculations," *Comput. Therm. Sci*., 4(4), pp. 297–315, (2012).
[17] Dombrovsky, L., Randrianalisoa, J., and Baillis, D., "Modified two-flux approximation for identification of radiative properties of absorbing and scattering media from directional-hemispherical measurements," *J. Opt. Soc. Am. A*, 23(1), pp. 91–98, (2006).
[18] Guo, Z. and Kumar, S., "Equivalent isotropic scattering formulation for transient short-pulse radiative transfer in anisotropic scattering plane layer," *Appl. Opt.*, 39(24), pp. 4411–4417, (2000).
[19] Wu, C.-J. and Ou, N.-R., "Differential approximation for transient radiative transfer through a participating medium exposed to collimated radiation," *J. Quant. Spectr. Radiat. Transf*., 73(1), pp. 111–120, (2002).
[20] Guo, Z., Aber, J., Garetz, B.A., and Kumar, S., "Monte Carlo simulation and experiments of pulsed radiative transfer," *J. Quant. Spectr. Radiat. Transf*., 73(2–5), pp. 159–168, (2002).
[21] Kim, K.H. and Guo, Z., "Ultrafast radiation heat transfer in laser tissue welding and soldering," *Numer. Heat Transf. A*, 46(1), pp. 23–46, (2004).
[22] Mishra, S.C., Chung, P., Kumar, P., and Mitra, K., "Development and comparison of the DTM, the DOM and the FVM formulations for the short-pulse laser transport through a participating medium," *Int. J. Heat Mass Transf*., 49(11–12), pp. 1820–1832, (2006).
[23] Singh, R., Mishra, S.C., Roy, N.K., Sekhawat, N.S., and Mitra, K., "An insight into the modeling of short-pulse laser transport through a participating medium," *Numer. Heat Transf.* B, 52(4), pp. 373–385, (2007).
[24] Muthukumaran R. and Mishra, S.C., "Interaction of a short-pulse laser of a Gaussian temporal profile with an inhomogeneous medium," *Numer. Heat Transf. A*, 53(6), pp. 625–640, (2008).
[25] Jaunich, M.K., Raye, S., Kim, K., Mitra, K., and Z. Guo, "Bio-heat transfer analysis during short pulse laser irradiation of tissues," *Int. J. Heat Mass Transf*., 51(23–24), pp. 5511–5521, (2008).
[26] Muthukumaran, R. and Mishra, S.C., "Transient response of a planar participating medium subjected to train of short-pulse radiation," *Int. J. Heat Mass Transf*., 51(9-10), pp. 2418–2432, (2008).
[27] Liu, L.H. and Hsu, P.-F., "Time shift and superposition method for solving transient radiative transfer equation," *J. Quant. Spectr. Radiat. Transf*., 109(7), pp. 1297–1308, (2008).
[28] Bhuvaneswari, M. and Wu, C.-Y., "Differential approximations for transient radiative transfer in refractive planar medium with pulse irradiation," *J. Quant. Spectr. Radiat. Transf*., 110(6-7), pp. 389–401, (2009).
[29] Ruan, L.M., Wang, S.G., Qi, H., and Wang, D.L., "Analysis of the characteristics of time-resolved signals for transient radiative transfer in scattering participating media," *J. Quant. Spectr. Radiat. Transf*., 111(16), pp. 2405–2414, (2010).
[30] Mishra, S.C., Muthukumaran, R., and Maruyama, S., "Comparison of the thermal effects of the transport of a short-pulsed laser and multi-pulse laser through a participating medium," *Int. J. Heat Mass Transf*., 55(21-22), pp. 5583–5596, (2012).
[31] Asllanaj, F. and Fumerou, S., "Applying a new computational method for biological tissue optics based on the time-dependent two-dimensional radiative transfer equation," *J. Biomed. Opt*., 17(7), paper 075007, (2012) (Erratum in *J. Biomed Opt*., 17(7), paper 079801, (2012)).
[32] Zhang, Y., Yi, H., and Tan, H., "One-dimensional transient radiative transfer by lattice Boltzmann method," *Opt. Expr*., 21(21), pp. 24532–24539, (2013).
[33] Bhowmik, A., Repaka, R., Mishra, S.C., and Mitra, K., "Analysis of radiative signals from normal and malignant human skins subjected to a short-pulse laser," *Int. J. Heat Mass Transf*., 68, pp. 278–294, (2014).

[34] Born, M. and Wolf, E., *Principles of Optics, Seventh (expanded) edition*, New York: Cambridge Univ. Press, (1999).
[35] Bohren, C.F. and Huffman, D.R., *Absorption and Scattering of Light by Small Particles*, New York: Wiley, (1983).
[36] Jacques, S. L., "Optical properties of biological tissues: a review," *Phys. Med. Biol*., 58, R37–R61 (2013).
[37] Scripov, V.P., *Metastable Liquids*, New York: Wiley, (1974).
[38] Dombrovsky, L.A., "Radiation heat transfer from a hot particle to ambient water through the vapor layer," *Int. J. Heat Mass Transf*., 43(13), pp. 2405–2414 (2000).
[39] Modest, M.F., *Radiative Heat Transfer, Third edition*, New York: Acad. Press, (2013).
[40] Farmer, J.T. and Howell, J.R., "Comparison of Monte Carlo strategies for radiative transfer in participating media," *Adv. Heat Transf*., 31, pp. 333–429, (1998).
[41] Dombrovsky, L.A. and Lipiński, W., "A combined P_1 and Monte Carlo model for multi-dimensional radiative transfer problems in scattering media," *Comput. Therm. Sci*., 2(6), pp. 549-560, (2010).
[42] Pustovalov, V.K., "Theoretical study of heating of spherical nanoparticle in media by short laser pulses," *Chem. Phys*., 308 (1-2), pp. 103–108, (2005).